Engineering Structures 193 (2019) 281–294

Contents lists available at ScienceDirect

Engineering Structures

journal homepage: www.elsevier.com/locate/engstruct

Wind-resistant design and safety evaluation of cooling towers by reinforcement area criterion

Miao Yu[a], Lin Zhao[a,b,*], Yanyan Zhan[a], Wei Cui[a,b,*], Yaojun Ge[a,b]

[a] State Key Lab of Disaster Reduction in Civil Engineering, Tongji University, Shanghai 200092, China
[b] Key Laboratory of Transport Industry of Wind Resistant Technology for Bridge Structures, Tongji University, Shanghai 200092, China

ARTICLE INFO

Keywords:
Large cooling tower
Interference criterion
Wind tunnel test
Finite element method
Dynamic reinforcement area
Extreme value reinforcement area envelope

ABSTRACT

Wind loads are the predominant loads of all the various loading combinations in structural design of cooling towers. Existing wind loading codes have a basic single interference factor and a simplified two-dimensional static wind pressure distribution formula, and do not enable accurate structural safety/reliability evaluation under dynamic wind loads. Among the various Equivalent Static Wind Loadings (ESWLs), the reinforcement-area-based ESWL is selected in this study, and the extreme reinforcement area considering wind directionality effect and nonuniform circumferential wind pressure is expressed as the equivalent criterion of reinforcement area envelope.

A structural safety evaluation method, based on this innovative cooling tower design criterion, is derived as the dynamic reinforcement area envelope concept. The effects of time-variant weighted internal forces and non-Gaussian peak factor for the reinforcement area envelope are considered. The reinforcement area envelopes are compared with those from three different codes based on traditional simplified ESWLs. Finally, the results show that the existing loading codes do not cover the effects of interference amplification for structural safety. An alternative framework based on the reinforcement area criterion of weighted dynamic interval forces and its extreme value envelope are proposed, which can optimize both the economy and the structural safety design of cooling towers.

1. Introduction

Large cooling tower structures are large-span, high-rise, spatial, thin-wall structures. Wind loads on large cooling towers are often considered as the predominant load of all load combinations in the design process [1]. In 1965, three cooling towers in the leeward region of a group of eight towers collapsed during only a five-year-return-period wind speed at the Ferrybridge Power Plant, UK [2]. Since then, wind-induced interference effects of tower groups have attracted a lot of attention from wind engineering researchers. At first, interference effect criteria for grouped cooling towers were determined at the load level. A grouped-tower interference factor was derived from wind pressure records obtained from field measurements or wind tunnel tests [3]. Then, with increasing computing power, interference criteria were developed to the internal forces level. Static or dynamic loads from wind tunnel tests were applied in finite element method (FEM) models to calculate internal forces and stresses [4,5]. Some scholars have focused more on evaluation of loading parameters and have tried to determine subtle changes of structural wind-induced effects with interference more accurately [6,7,9]. The interference criteria are usually defined based on several levels, involving wind loading, wind induced displacement or internal forces. The interference factor is related with amplification effects of static wind loadings from the neighboring terrain or building, and the wind-induced vibration coefficient is used to evaluate dynamic response due to the incoming turbulence. In recent years, interference criteria for weighted internal forces or reinforcement ratio, according to conditions of multiple wind flow directions, have been proposed to achieve uniformity of various existing evaluation standards [10]. Coefficients based on the concept of the structural reinforcement area can reflect structural behavior under complex interference conditions. Representative progress in recent decades are shown in Table 1.

Tower group interference criteria are derived from indicators of loads and internal forces, which can partially reveal structural dynamic properties under wind loads. However, interference effects are usually affected by multiple factors such as the number of towers, tower layout, and distance between towers. The distribution of wind pressure on tower surfaces is too sensitive and diverse to be expressed accurately by

* Corresponding authors at: State Key Lab of Disaster Reduction in Civil Engineering, Tongji University, Shanghai 200092, China.
E-mail addresses: zhaolin@tongji.edu.cn (L. Zhao), cuiwei0322@qq.com (W. Cui).

https://doi.org/10.1016/j.engstruct.2019.05.031
Received 21 October 2018; Received in revised form 15 April 2019; Accepted 12 May 2019
Available online 21 May 2019
0141-0296/

Table 1
Typical progress in interference effects among grouped buildings.

Reference	Year	Methods	Towers layout	Selected criteria
Sun and Gu	1995	Wind tunnel test	Two and four tower combination	Drag coefficient, lift coefficient, mean pressure distribution
Niemman and Kopper	1998	Wind tunnel test	Towers group and adjacent buildings	Maximum tensile meridional force
Orlando	2001	Wind tunnel test + FEM analysis	Two towers	Mean meridional force, mean hoop bending moment, maximum hoop and meridional normal stresses
Ke et al.	2013	Wind tunnel test	Isolated tower	Equivalent static wind loads internal force component
Uematsu et al. [8]	2014	Wind tunnel test + FEM analysis	Open-topped oil storage tanks	Mean internal and external pressure coefficients, buckling loads
Zhang et al.	2017	Wind tunnel data + FEM analysis	Six-tower combination	Average wind load parameters, peak displacement factor
Zhao et al.	2018	Wind tunnel data + FEM analysis	Six-tower combination	Reinforcement in the three-dimensional static wind load

a single coefficient or a simple formula. Some equivalent wind load distribution patterns often rely on evaluation processes with different indicators. Using the concept of structural reinforcement area as an evaluation criterion can cover the comprehensive effects of a variety of internal force indicators. Some preliminary investigations have implemented the strategy of selecting reinforcement area criteria with interference conditions. However, only equivalent static wind load (ESWL) applied to cooling towers under complex combinations have been achieved [10]. With this method, static wind load calculations are based on average wind loads obtained from wind tunnel tests, and the influence of different tower group interference conditions on the structure are considered. Although this is some improvement over the traditional simplified amplification factors (such as interference factor and wind-induced vibration factor, etc.) [11] from codes, the 2-D wind pressure distribution mode by codes is still adopted, rather than 3-D ESWL, and the influence of tower group interference effects on fluctuating wind loads are ignored.

With respect to the pressure-measurement equipment in the wind tunnel test for tower group combinations and transient response analyses in the time domain considering various interfering aerodynamic loadings, a novel concept and corresponding algorithm of time-variant dynamic reinforcement area reflecting the effects of weighted internal forces is introduced. This algorithm takes into account the interference's influence on the static and fluctuating wind pressures on cooling towers, and then corresponding 3-D ESWL can be summarized based on the Extreme Reinforcement Area Envelope (ERAE) for time-variant reinforcement area for multiple wind directions. By comparison between the simplified specifications from the codes and the full transient dynamic internal force calculation, it can be proved that ERAE from the time-variant dynamic calculation reflects the tower group interference effects more accurately, and is defined as a universal ESWL criterion for cooling tower structural design [12]. The algorithm of ERAE and its ESWL can be defined as the most realistic loading pattern in design of cooling towers, which can deal with the diversity of evaluation criteria and discreteness of wind pressure distributions under interference conditions.

The research is divided into three main stages. First, static and dynamic wind pressure data for cooling towers are obtained through synchronous pressure-measured wind tunnel tests. Second, the time-variant internal forces of the structure can be calculated by the full-transient dynamic analysis utilizing the measured wind loads process. Then, the dynamic reinforcement area is derived using the proposed algorithm considering the criteria for weighted time-variant internal forces through the finite element method. Finally, considering structural reliability redundancy, the peak value of the dynamic reinforcement area in the vertical direction for a single wind angle can be obtained for the structural time-variant dynamic reinforcement area for circular elements at different elevations, and an ERAE curve can be obtained by combining multiple flow conditions. Fig. 1 illustrates the main work flow chart in this study.

2. Theoretical background of numerical simulation

2.1. POD-based dynamic load interpolation algorithm

Through the Proper orthogonal decomposition (POD) method, time-variant taps measured wind pressures during the test, which are converted into the time-variant wind loads on all nodes of the cooling tower finite element model. The wind pressure field is reconstructed using a small number of low-order eigenmodes by this method, which can retain most of the pulsating energy [13]. Thus, the wind pressure function $P(x, y, t)$ is decomposed into only position-dependent eigenvectors and time-dependent principal coordinate functions, where x, y represent position coordinates and t represents time.

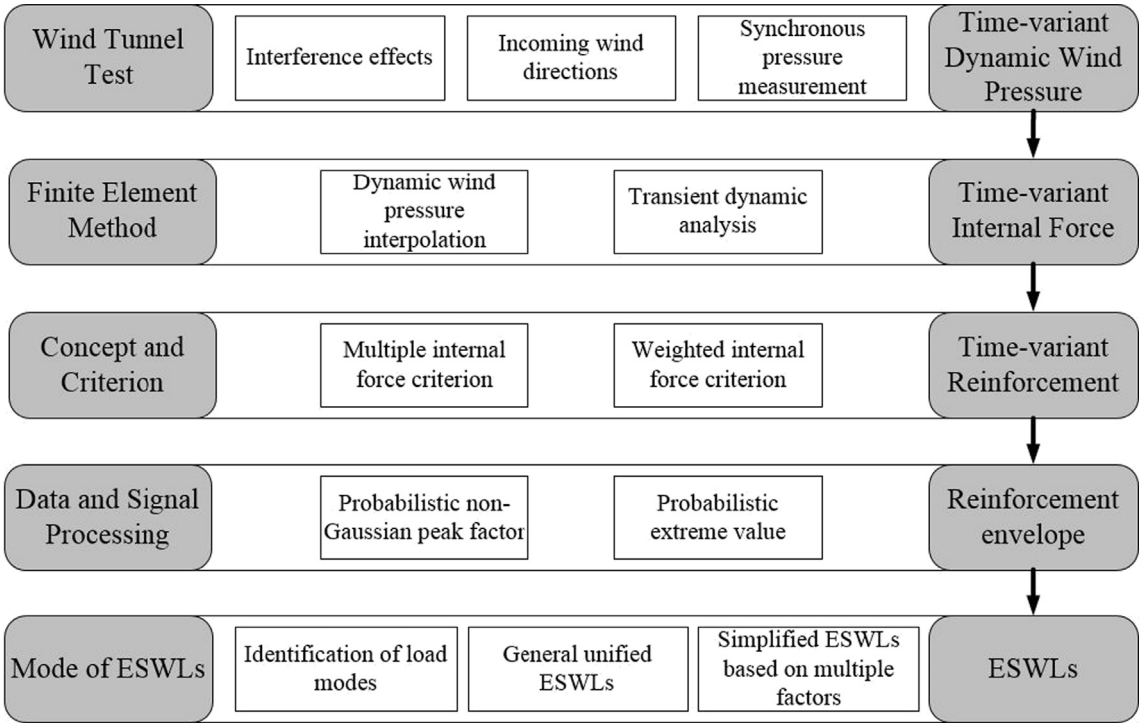

Fig. 1. Main work flow chart.

$$P(x, y, t) = \sum_{n} \phi_n(x, y) a_n(t) \tag{1}$$

The eigenvectors $\phi(x, y)$ can be obtained from:

$$[C]\{\phi(x, y)\}_n = \lambda_n \{\phi(x, y)\}_n \tag{2}$$

where $[C]$ is the wind pressure covariance matrix, λ_n is the eigenvalue, and the main coordinate function can be obtained from:

$$\{a(t)\} = [\Phi]^T \{P(x, y, t)\} \tag{3}$$

By interpolating the eigenvectors and then using Eq. (1), the time-variant wind pressure at unmeasured points can be interpolated. Then the concentrated load at each node in the finite element model is formed by Eq. (4). The integrating function $f(u, h, \theta)$, u, h, θ represents the parameters related to average wind speed, wind profile index and projection direction vector, respectively.

$$WL(t) = \iint P(x, y, t) f(u, h, \theta) dxdy \tag{4}$$

2.2. Time-variant reinforcement area

The reinforcement area can be calculated considering the time-variant internal forces for each element aiming at the eccentric compressed concrete element according to the Chinese design code. To obtain the time-variant element reinforcement area, the code formulas [14] for the reinforcement calculation for each element are:

$$N_b(t) = \alpha_1 f_c b x(t) \pm f'_y A'_s(t) \pm f_y A_s(t) \tag{5}$$

$$N_s(t) = \alpha_1 f_c b x(t) \pm f'_y A'_s(t) \pm \sigma_s(t) A_s(t) \tag{6}$$

$$M(t) = \alpha_1 f_c b x(t) \left(h_0 - \frac{x(t)}{2}\right) \pm f'_y A'_s(t)(h_0 - a'_s) \tag{7}$$

$$\sigma_s(t) = E_s \varepsilon_{cu} \left(\frac{\beta_1}{\xi(t)} - 1\right) \tag{8}$$

In these formulas, $N_b(t)$ is the large eccentric axial compression force per unit length, $N_s(t)$ is the small eccentric axial compression force per unit length, $M(t)$ is the bending moment per unit length, f_c is the compressive strength of selected concrete types, and b is the width of a section with unit length. f_y and f'_y are the design values of tensile and compressive strength of steel reinforcement, respectively; $\sigma_s(t)$ is the steel tensile stress near the neutral layer before yield strain is reached, and h_0 is the effective height of the cross-sectional compression zone, which is obtained by converting the wall thickness at different positions. E_S is Young's modulus for steel, ε_{cu} is ultimate steel strain, $\xi(t)$ is compression zone height, $A_s(t)$ is the time-variant reinforcement area of the outside shell, and $A'_s(t)$ is the time-variant reinforcement area of the inside shell. Fig. 2 shows the force equilibrium diagram of the eccentric compressed concrete member and the definition of each symbol in Eqs. (5)–(8). The calculated reinforcement area is defined as the reinforcement area divided by each unit length area. There are four types of reinforcement elements in the inner and outer sides in the meridional and circumferential directions, namely inside circumferential reinforcement, outside circumferential reinforcement, inside meridional reinforcement and outside meridional reinforcement, indicated hereafter by R_{CI}, R_{CO}, R_{MI}, R_{MO}, respectively.

2.3. Extreme reinforcement area

Probabilistic statistics are employed at the rate guaranteed to calculate the extreme value reinforcement for each element. For convenience, the peak factor method is used to evaluate the extreme reinforcement area, which depends on probabilistic distributions of dynamic reinforcement area. For the Gaussian distribution, the Gust Loading Factor method [15], shown in Eq. (9), is widely used. For the non-Gaussian distribution, the "Hermite method" [16] is used to apply the classical peak factor method to the non-Gaussian process, referred in Eq. (10).

$$g = (2 \ln \nu_0 T)^{1/2} + \frac{\gamma}{(2 \ln \nu_0 T)^{1/2}} \tag{9}$$

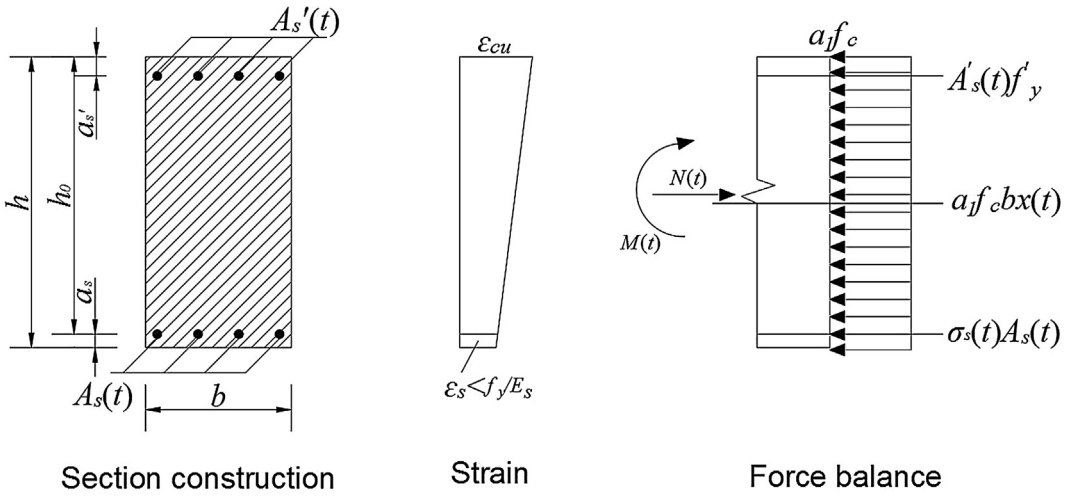

Fig. 2. Schematic diagram of force on eccentric compression element.

$$g = \kappa\left\{\left(\beta + \frac{\gamma}{\beta}\right) + h_3\left[\beta^3 + 2\gamma - 1 + \frac{1.98}{\beta^2}\right] + h_4\left[\beta^3 + 3\beta(\gamma - 1) + \frac{3}{\beta}\left(\frac{\pi^2}{6} - \gamma + \gamma^2\right) + \frac{5.44}{\beta^3}\right]\right\} \quad (10)$$

in which g is the peak factor, v_0 is the zero-crossing rate of the Gaussian process, T is the observation time interval, $\gamma = 0.5772$ is Euler's constant, and parameter $\beta = \sqrt{2\ln(v_0 T)}$. Other parameters in Eq. (10) are omitted here for brevity and can be found in Ke et al. [16]. According to the results from the above algorithms, when the peak factor is 2.5, structural reliability can reach over 95%. In the process of dealing with the time-variant element reinforcement area, peak factor value 3.5 is taken to ensure that structural safety reliability can reach over 99% by considering the probability reliability requirement method, expressed in Eq. (11). Eq. (11) is also used to obtain the element reinforcement envelope value.

$$A_{ep} = A_{mean} + gA_{std} \quad (11)$$

where A_{ep} is the element reinforcement area envelope value, A_{mean} is the mean value of the time-variant element reinforcement area and A_{std} is the standard deviation of the time-variant element reinforcement area.

2.4. Reinforcement area envelope considering multiple wind directions

The extreme reinforcement area for each element can be obtained from Eq. (11). Thus, the reinforcement area envelope along the tower height can be derived considering reinforcement fluctuation in the circumferential direction and various wind directions. The main process is summarized by Eq. (12).

$$A_{epl} = f_n[A_{ep}(t, h, \theta)_{max}]_{max} \quad (12)$$

where t is time, θ is circumferential angle, h is elevation, and f_n is the extreme value function to get the maximum reinforcement area under different circumferential angles and wind loading angles. First, using the three parameters t, θ, h, a maximal extreme value curve for a certain wind direction can be found. Then, R_{CI}, R_{CO}, R_{MI}, R_{MO} along the height of a cooling tower under various wind angles by the function f_n can finally be achieved.

3. Dynamic wind pressure under complex tower group combination

Pressure-measured wind tunnel experiments were conducted in the TJ-3 wind tunnel to get the dynamic wind pressure distribution. The test section size of the wind tunnel is 14 m (length) × 15 m (width) × 2 m (height). The wind speed range in the wind tunnel is 1–17.6 m/s, and is continuously adjustable. The flow field non-uniformity index $\delta U/U \le 1.9\%$, turbulence intensity $I_u \le 2.0\%$, vertical flow inclination angle $\Delta\alpha \le \pm 0.2^\circ$, and horizontal deviation angle $\Delta\beta \le \pm 0.1^\circ$. Fig. 3 shows the flow field simulation using spires and blocks on the ground. In Fig. 3, Z_G represents wind speed at gradient wind height, U_G represents gradient wind height, $I_u(z)$ represents turbulence intensity, and $U(z)$ is mean wind speed at elevation z.

The cooling tower is 185 m high and its other key dimensions are shown in Fig. 4. The height of the tower exceeds the restrictions in the current Chinese Code [11] on cooling tower height, and the interference effects due to the surrounding terrain and the arrangement of nearby tall buildings and towers cannot be ignored. Therefore, it is necessary to perform wind tunnel tests to ensure the safety of the cooling tower structure. Considering both blockage limit and Reynolds number effect simulation, eight rigid tower models at a 1:300 scale were adopted. The projected area of the whole tower group model in the along-wind direction was approximately 1.47 m^2, and the maximal block ratio was approximately 4.9%. The use of plexiglass 3 mm thick as the model construction material ensured the model's rigidity during the experiment, so that the deformations would not exceed the allowable range. Fig. 5 shows the simulated self-power spectra of the incoming flow. Accordingly, it can be seen that under the experimental conditions, the wind spectra of the along-wind direction and the cross-wind direction are in good agreement with several codes' spectra. In the wind spectrum, Z represents the turbulent integral scale and U represents the wind speed.

As shown in Fig. 6, a total of 16 × 36 = 576 measurement points were arranged on the inner and outer surfaces of the model to be tested. On the outer surface, 12 layers of measurement points were arranged at different heights in the meridional direction, and are shown in Fig. 6(a). In the circumferential direction, taps were evenly arranged at intervals of 10°, so each layer had a total of 36 pressure measurement points, numbered 1–36. A total of 432 measurement points was arranged on the outside shell. 4 layers of measurement points were arranged on the inner surface in the meridional direction (respectively on the 2nd, 5th, 8th, and 11th layers corresponding to the points on the outer surface). The circumferential arrangement was the same as for the outer surface. The inner surface had 36 × 4 = 144 measuring points. The pressure measurement frequency was 300 Hz and the sampling time was 60 s. Fig. 6(b) shows an isolated tower pressure-measured model installed in the TJ-3 wind tunnel.

The Helmholtz effects for the tubes connecting pressure taps is an

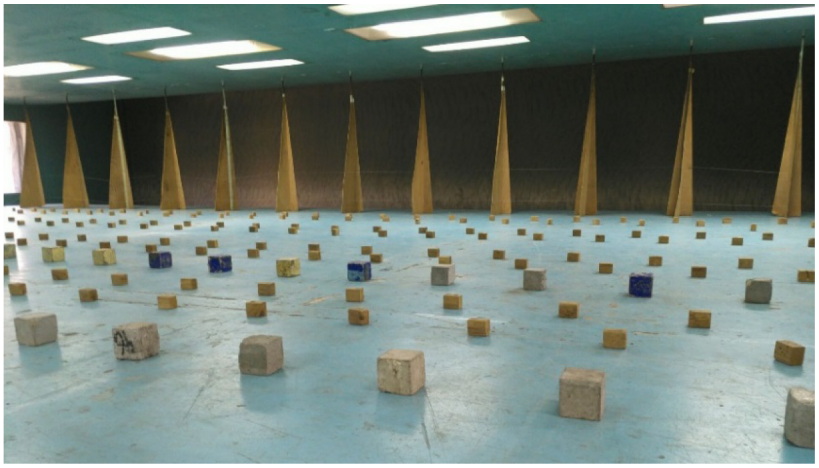

a) Grids and blocks in TJ-3 wind tunnel

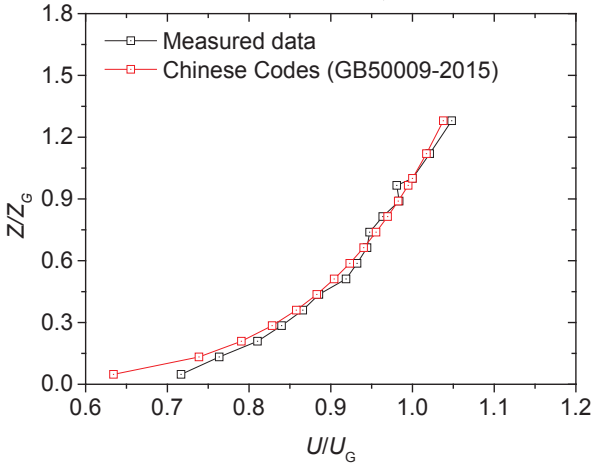

b) Average wind velocity profile

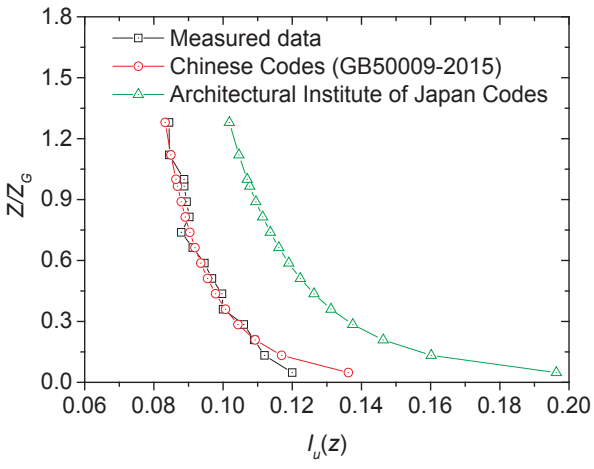

c) Turbulence intensity profile

Fig. 3. Wind field simulation in wind tunnel.

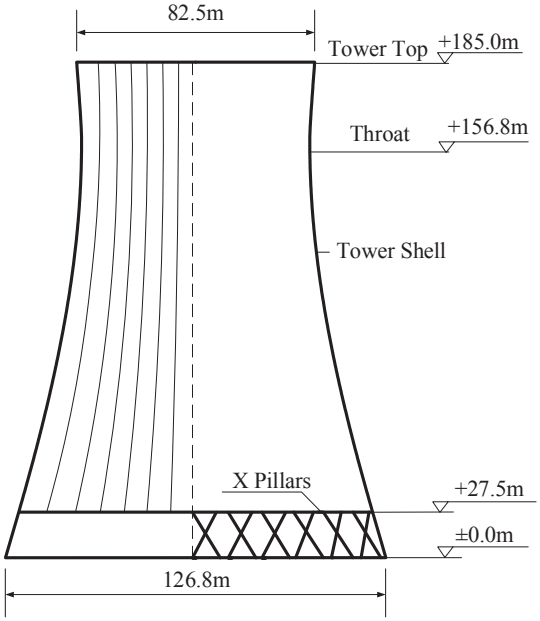

Fig. 4. Schematic diagram of cooling tower.

importance influence factor during the design of wind tunnel experiments. For the same length (70 cm) of pressure tubes used in the experiment, we measured and corrected the phase lag and amplitude at different frequencies by means of instrument calibration (see Fig. 7). The correction method is described in Hu et al. [18] in detail.

To compensate Reynolds number effect, various roughness elements were placed on the tower model. Four different wind speeds of 6–12 m/s and four different roughness element sizes were employed in the wind tunnel test to ensure the measured mean pressures matched the code values, as shown in Fig. 8. With 0.4 mm rough element (RE) size, the results almost matched the code values at a wind speed of 8 m/s. On the other hand, the fluctuating wind pressure coefficients were compared with previous field wind pressure measurement results of a super-tall cooling tower under turbulent wind [19]. The fluctuating wind pressure coefficients on the windward side are slightly larger than the actual measured values, but the maximum RMS values are basically similar. It is reasonable to assume that wind pressure distribution and the wind flow field simulated in the wind tunnel is more conservative than the actual situation from the safety viewpoint.

In the wind tunnel test, the experimental results for the eight-tower combination in rhombus arrangements are generally considered to be more unfavorable than those in rectangular or linear arrangements [10]. Fig. 9 illustrates the rhombus arrangement and defines the wind directions. The range of wind angle β changes for 16 wind directions from 0° to 337.5° with 22.5° increments. It is usually known that the tower on the leeward side is more unfavorable in the rhombus

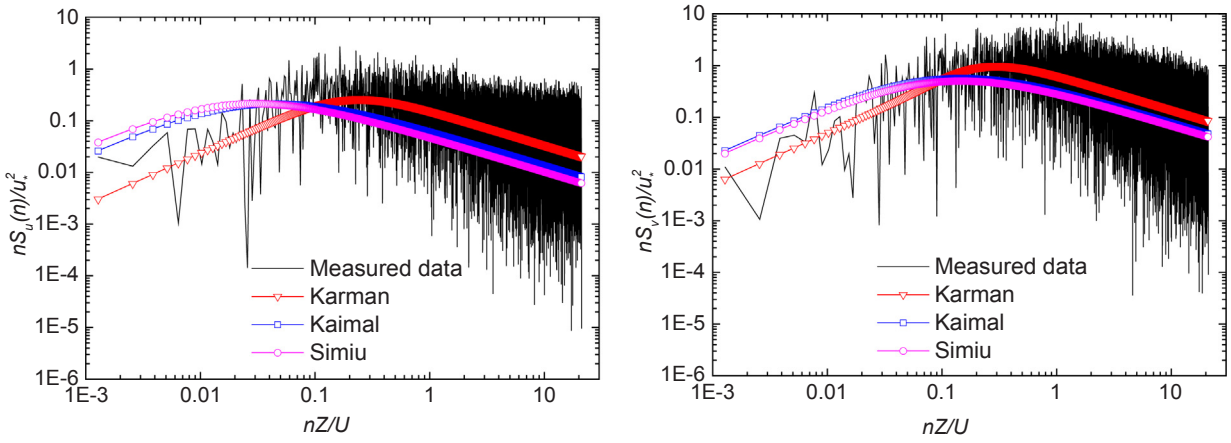

Fig. 5. Comparison between measured wind spectrum and target spectrum function [17].

arrangement, and the wind-induced accident at the Ferrybridge Power Plant, UK shows the same conclusion. After preliminary processing and calculation of the experimental results, the rhombus-arranged T3 tower at 180°wind direction was shown to be the worst condition when the inference criterion at the load level was employed, so T3 tower was selected as the study object in the following sections. The tower group interference factor (IF) in this condition obtained from the comparison with an isolated tower in terms of the mean value of the structural overall resultant base force is 1.231, and the corresponding state is defined as the "narrow channeling" condition.

4. Effects of multiple loading combination

The transient wind loading obtained from the wind tunnel test is applied in the FEM model and other loading effects (such as dead load, temperature, seismic action, etc.) specified by the code are also

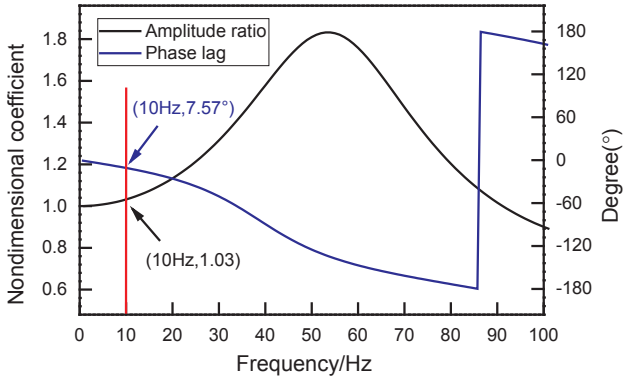

Fig 7. The amplitude ratio and phase lag caused by the length of pressure tube.

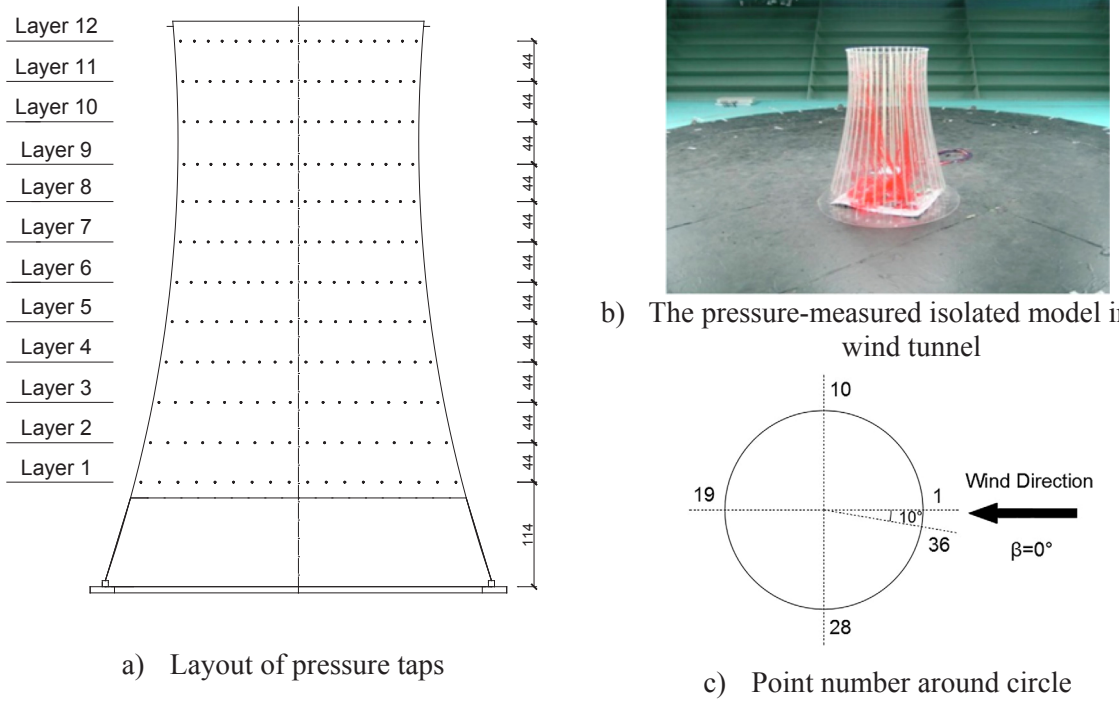

Fig. 6. Layout of pressure taps on cooling tower model (Unit: mm).

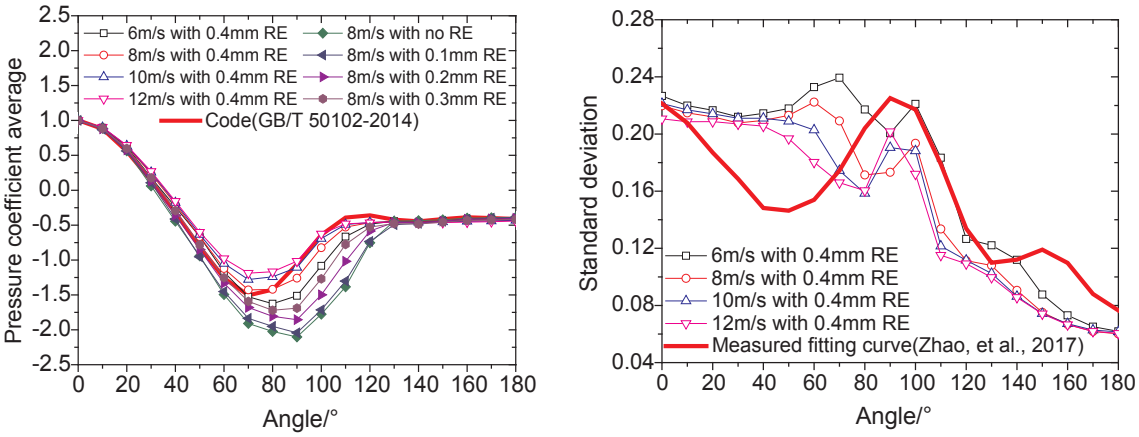

a) Mean value of pressure coefficient

b) RMS of pressure coefficient

Fig. 8. Experimental model wind pressure distribution simulation under high Reynolds number conditions.

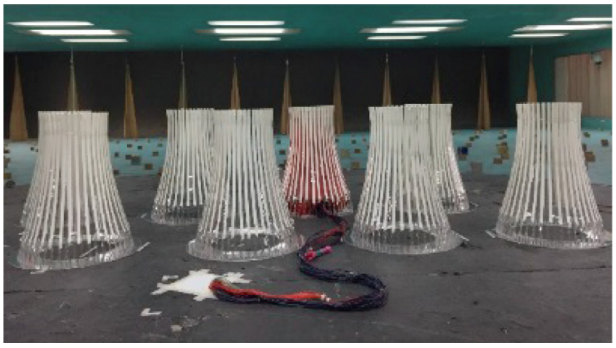

a) Eight-tower rhombus arrangement

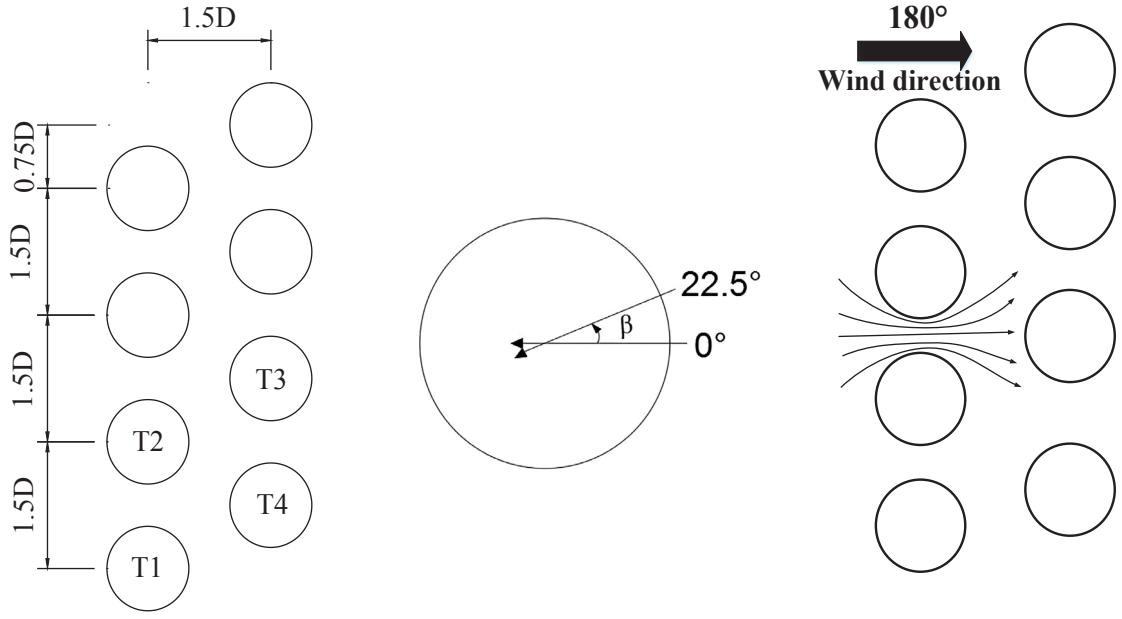

b) Tower number definition

c) Wind direction definition

d) "narrow channeling" condition

Fig. 9. Eight-tower rhombus arrangement and wind direction definition.

considered. The transient internal forces under different loading combinations can be computed from the FEM model. The outer envelope of the time-variant dynamic reinforcement area is obtained from Eqs. (5)–(8) above and employed as the evaluation criterion for the safety performance of the cooling tower. This criterion is accurate enough for analyzing the tower group influence effects and the turbulent wind effects on the cooling towers.

The FEM analysis of the cooling tower structure utilized the commercial software ANSYS, 14.0. During the FEM modeling, the cooling tower ventilator and the herringbone pillars were discretely modeled using Shell63 element and a beam is modeled using Beam188. The material properties of shell elements are made of concrete of the same grade as the actual cooling tower, where the elastic modulus is 30 kN/m^2 and Poisson's ratio is 0.2. The tower base was constructed as 48 pairs of X-shaped pillars. The pillar bottoms were rigidly connected to a ring base. Each group of pillars divided the bottom of the column into 1 group of ring base units. Each group of ring base units applied a set of 6-degree-of-freedom equivalent stiffness spring constraint (Combin14) to simulate group pile effects and the structure-foundation-soil coupling effect. Then the equivalent soil spring stiffness coefficient can be calculated based on the field measured data according to the *M* method given in the Codes [20]. The simulated stiffness of the soil spring in this method is widely acknowledged and normally matches real conditions. There are 5809 nodes in the tower of the structural FEM model. There are 96 elements in the circumferential direction, 54 elements in the meridional direction, and a total of 5184 shell elements with a total of 31,104 degrees of freedom. For the mesh size, the smallest mesh size is about 1.29 m × 2.8 m and the maximum is about 2.07 m × 3.0 m. The FEM model meshing details are shown in Fig. 10. The fundamental frequency of the natural vibration mode of the finite element structural model is 0.83 Hz. The mode shapes is shown as Table 2.

According to the wind tunnel test results, the time-variant wind pressures from the POD method at the 36 × 12 measurement points were interpolated and expanded to 96 × 55 nodes in the FEM model, and the decomposed wind loads were applied in the FEM model. The transient force analysis was implemented to get the time-variant internal forces. The calculation process had a total of 3000 time steps. The time steps were determined by the geometry scale, sampling frequency, and wind speed, and then corrected by the *St* number [21]. The time step employed in this study was 0.167 s.

Table 2
Mode shapes of the cooling tower.

Frequency (H_Z)	0.83	0.85	0.89	1.65
Mode Shape	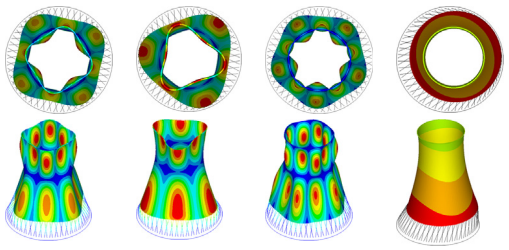			
Mode number	1, 2	3, 4	5, 6	35, 36
Circumference & Meridian harmonic number	4 and 2	3 and 2	5 and 2	Global lateral bending

Table 3
Loading combination definitions.

No.	Loading combinations	No.	Loading combinations
1	$1.0S_G + 1.4\ S_W + 0.6\ S_{WT}$	8	$1.0S_G + 0.6S_W + 0.6\ S_{WT}$
2	$1.0S_G + 1.4\ S_W + 0.6\ S_{ST}$	9	$1.35S_G + 1.4S_W + 0.6\ S_{ST}$
3	$1.0S_G + 0.84S_W + 1.0\ S_{ST}$	10	$1.2S_G + 1.4S_W + 0.6\ S_{ST}$
4	$1.0S_G + 0.84S_W + 1.0S_{WT}$	11	$1.1S_G + 0.526S_W + 0.6\ S_{ST}$
5	$1.0S_G + 1.0\ S_W + 0.6\ S_{ST}$	12	$1.2S_G + 0.84S_W + 0.6\ S_{ST}$
6	$1.0S_G + 1.0S_W + 0.6\ S_{WT}$	13	$1.35S_G + 0.35S_W + 0.6\ S_{ST} + 1.3\ S_{Ehk} + 0.5S_{Evk}$
7	$1.0S_G + 0.6S_W + 0.6\ S_{ST}$	14	$1.0S_G + 0.35S_W + 0.6\ S_{ST} + 1.3\ S_{Ehk} + 0.5S_{Evk}$

Note: S_G, S_W, S_{ST}, S_{WT}, S_{Ehk}, and S_{Evk} are load effects related to gravity, wind, summer temperature, winter temperature, horizontal seismic action and vertical seismic action, respectively

The time-variant internal forces were used to calculate R_{CI}, R_{CO}, R_{MI}, and R_{MO} using Eqs. (5)–(8) of the cooling towers according to the current China Concrete Structural Design Code [14]. It is worth mentioning that the seismic load, as a dynamic load, usually has an impact

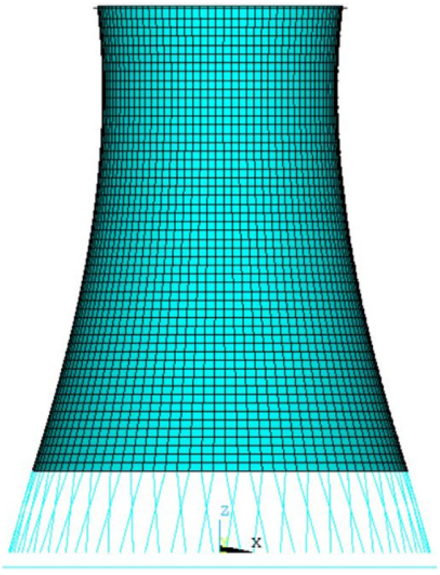

a) Finite element model

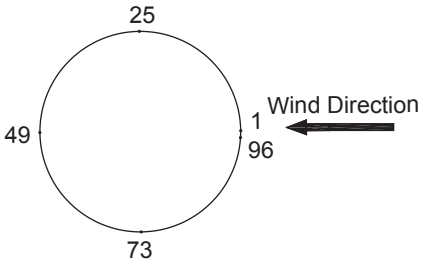

b) Element numbers along the circular

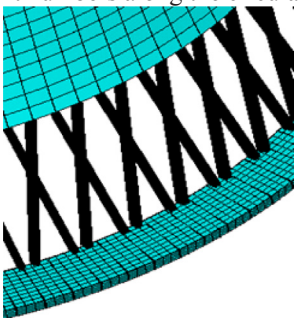

c) Ring base in detail

Fig. 10. FEM model of cooling tower.

Table 4
Instructions for other load categories applied to cooling towers.

Loading type	Parameters	Value	Loading type	Parameters	Value
Full-scale wind load	Design wind speed	37.2 m/s	Earthquake action	Seismic intensity	7
	Wind profile power exponent	0.15		Feature cycle	0.45 s
Temperature load	Summer temperature difference	15 °C		Damping ratio	0.05
	Winter temperature outside	−29.2 °C		Basic earthquake acceleration value	0.1 g
	Winter temperature inside	38.8 °C		Horizontal seismic influence coefficient	0.08

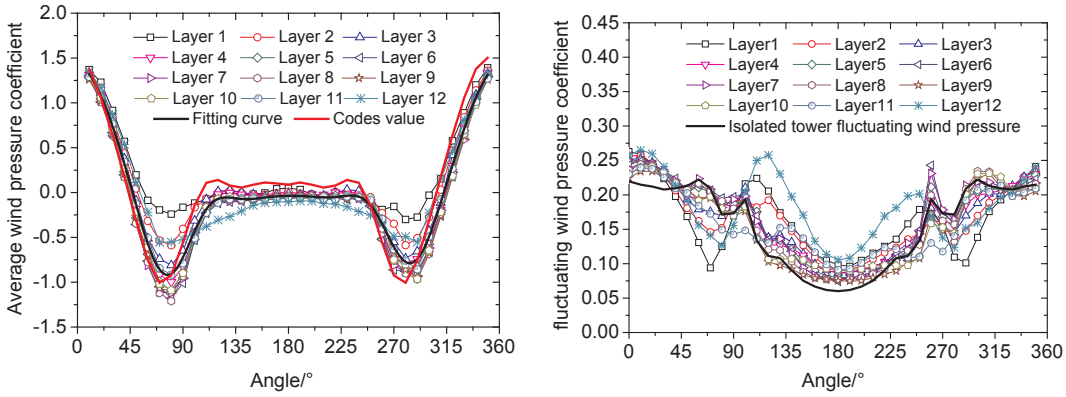

a) Average wind pressure coefficient b) Fluctuating wind pressure coefficient

Fig. 11. Comparison of wind pressure coefficients at different heights.

on the boundary areas between the superstructure and the substructure [22]. In the structural design of cooling towers, necessary attentions are focused on the effects of soil-pile-structure interaction on the seismic response of cooling towers. Though the seismic effects exceed the scope of this study, the seismic load combination is still taken into account by seismic response spectrum method. The 14 combinations of internal forces considered during the reinforcement process are shown in Table 3. Table 4 shows other load categories involved during the loading combination.

5. Wind load characteristics and structural dynamic performance

For the experimental results of the "narrow channeling" condition, the initial average wind pressure coefficients and the fluctuating wind pressure coefficients were as illustrated in Fig. 11. The polynomial fitting results considering the asymmetry pressure distribution for wind pressure and code values are also shown. Eq. (13) shows the polynomial fitting function considering asymmetry. Table 5 shows the relevant parameters obtained by the fitting process.

$$C_P(\theta) = \sum_{i=0}^{7} a_i \cdot \cos i\theta + \sum_{i=1}^{7} b_i \cdot \sin i\theta \tag{13}$$

The interferences at the bottom and the top of the tower are more obvious, and there is a great difference compared with other layers' average wind pressure. The asymmetrical average wind pressures due to circumferential interference are also clearly shown in Fig. 11.

Table 5
Relevant parameters obtained by fitting process.

Parameters	Values	Parameters	Values
a_0	0.015	b_1	−0.033
a_1	0.389	b_2	−0.001
a_2	0.657	b_3	0.021
a_3	0.398	b_4	0.013
a_4	−0.006	b_5	−0.005
a_5	−0.09	b_6	−0.006
a_6	0.017	b_7	0.0002
a_7	0.026		

Compared with the maximal standard deviation of the fluctuating wind pressure coefficients in the throat position of the isolated tower, the values on the windward and leeward sides at all different elevations along the tower under the interference conditions are obviously greater. This shows that the distribution of fluctuating wind pressure is obviously different from that of the isolated tower due to the interference effect, and the fluctuating wind pressure under the interference conditions increases for most tower parts. This phenomenon is more obvious on the windward side, which will control the structural design. This is more obvious at the upper part than at the lower part of the tower.

It can be concluded that simply adopting the two-dimensional symmetrical wind pressure from the loading codes and ignoring the interference effects on the average and fluctuating wind pressure makes the tower structure more vulnerable.

The nodal displacements were calculated for the "narrow channeling" condition using the transient dynamics calculation method. Fig. 12(a) shows the displacements at the throat position. The displacements on the windward surface are much larger than those on the leeward surface, and there are three extreme values on the windward surface and the lateral wind surface. The maximum displacement on the windward surface is close to 6 cm, and those at most nodes on the leeward surface are less than 1 cm. Through the gust loading factor method (GLF method), nodal displacements can be used to get wind-induced vibration coefficients based on Eq. (14) with the peak factor introduced in Chapter 2. Fig. 12(b) shows an expression for wind-induced vibration coefficient.

$$\beta = \frac{\bar{y} + \tilde{y}}{\bar{y}} = 1 + g\frac{\sigma_y}{\bar{y}} \tag{14}$$

When the mean displacement is small, the wind-induced vibration coefficients defined by the GLF method give larger values, usually greater than 4.0, which cannot reasonably reflect the structural performance. For the GLF method, it is not easy to judge whether it is ineffective or not while calculating the wind-induced vibration

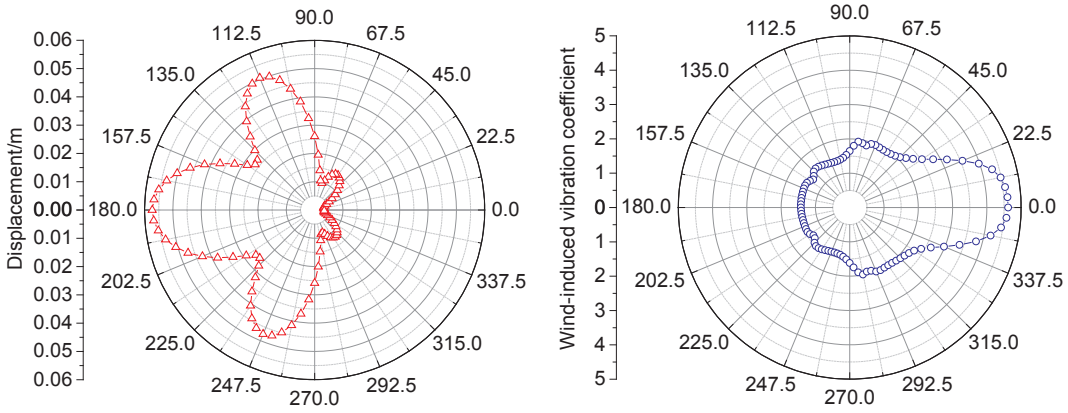

a) Mean displacement b) Wind-induced vibration coefficients

Fig. 12. Mean displacement response and wind-induced vibration coefficient at throat part.

coefficient, which prevents reasonable engineering application due to the existence of many positions with smaller mean value responses.

By extracting the internal forces induced by wind loads, it can be seen that the circumferential bending moments show drastic fluctuations, as shown in Fig. 13 as an example. In Fig. 14, the comparison of the standard deviation of the circumferential bending moments of the isolated tower and the "narrow channeling" condition related to the tower height shows obvious interference effects at the internal force level. In fact, the same conclusions can be made for the meridional and circumferential axial internal forces. Furthermore, structural design of cooling towers based on the equivalent static force method still ignores the complex variation of static and dynamic wind loading due to interference effects and three-dimensional end effects. The relatively complex fluctuations for structural responses of cooling towers in the time history cannot be reasonably illustrated by simplified loading parameters such as IF values and wind-induced vibration coefficients.

Due to the variety of structural internal forces and their directionality, especially with the different interference effects, the internal force effects are very variable. The IF or the wind-induced vibration coefficients from a single kind of internal force cannot be used to evaluate structural design safety. The code method has shown its inapplicability at the internal force level. According to the internal force envelope under "narrow channeling" condition, the code internal force criterion is insufficient in the lower middle areas, while creating redundancy in other areas. Due to the variety of internal forces, it is difficult to find a suitable kind of internal forces to meet the overall requirements without causing redundancy. As shown in Fig. 15, the circumferential bending moments give the comparison between the internal forces calculated by the transient dynamic method and the code method.

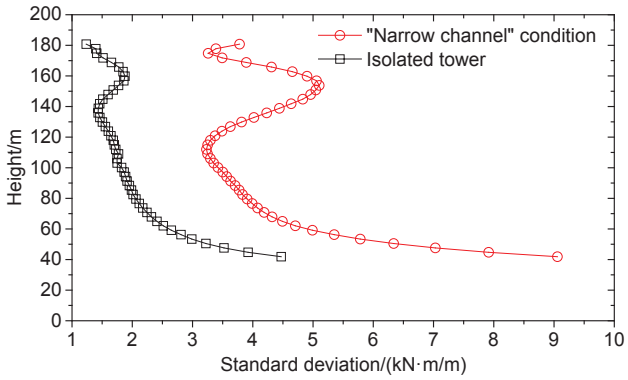

Fig. 14. Height-dependent circumferential bending moments for "narrow channeling" and isolated tower condition.

The wind-induced vibration coefficients obtained from codes are usually evaluated at the internal force level. However, the data obtained by transient dynamic method are analyzed at the internal force level, which are more dispersed and fluctuate dramatically around the mean values. Therefore, the wind-induced vibration coefficients obtained by the GLF method are invalid for design of structures. Fig. 16 shows the height- and direction-dependent wind-induced vibration coefficients for the "narrow channeling" condition. Fig. 16(b) shows that the wind-induced vibration coefficients are different for different internal force criteria. As a result, it is still unknown how to choose evaluation criteria to ensure the precision and effectiveness of equivalent wind loading factors at the internal force level. In the next section,

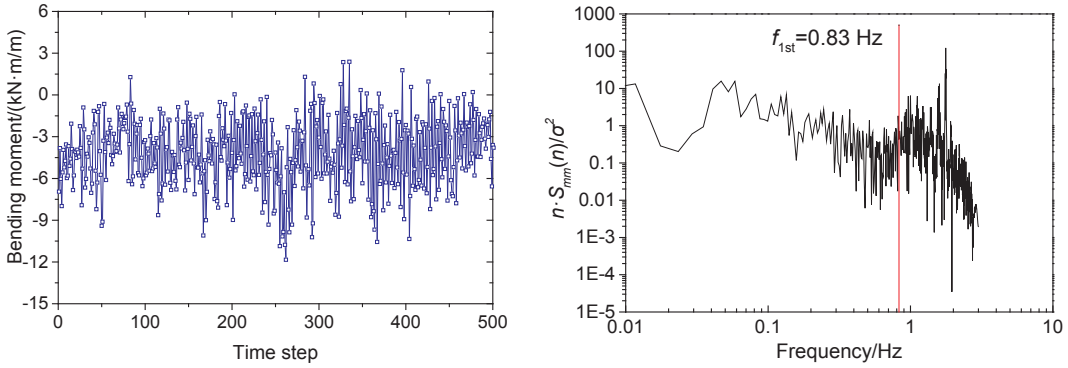

a) Time-variant bending moment b) PSD of bending moment

Fig. 13. Wind-induced circumferential bending moments of windward point at throat.

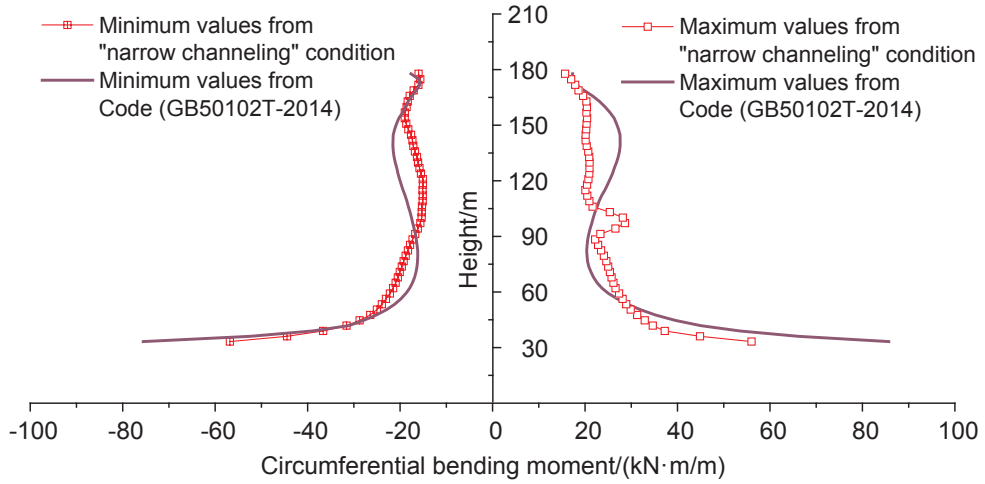

Fig. 15. Comparison of extreme values of height-dependent circumferential bending moment between tests and code.

an innovative evaluation criterion is proposed to overcome this dilemma.

6. Safety evaluation criterion

Since the evaluation criteria for cooling tower performance differ greatly in quantifying the interference effects of tower groups [10], it is difficult for the evaluation criteria for internal force levels and displacement levels for cooling towers to cover all the extreme states. Therefore, it is necessary to build an internal force weighted criterion to cover the various internal forces and to eliminate invalid vibration coefficients with smaller mean values. In this section, criteria of time-variant reinforcement area statistics indices for tower group interference effects are proposed. The algorithm for calculating time-variant reinforcement area is expressed by Eqs. (5)–(8). From these expressions, the different internal forces can be applied to the reinforcement area as the weighting factor, which has deterministic physical meaning.

The time-variant reinforcement area under “narrow channeling” conditions is computed at 2000 time steps after reaching a stationary state during the transient dynamic, as shown in Fig. 17. By comparing the reinforcement areas over the entire tower, it is considered that the time-variant reinforcement in the throat position can describe the changes of the whole tower in the different circular directions and in the time history.

Under the “narrow channeling” condition, the circumferential number of 49 is at the windward surface, which is chosen as the representative element to display the meridional reinforcement area fluctuation in Fig. 17(d). In Fig. 17(c), the circumferential No.30 element with maximum circumferential reinforcement area is selected to show the fluctuation over time.

Even at this reinforcement level, the time-variant reinforcement changes are still great. Fig. 17 shows that the circumferential reinforcement area has significant fluctuations over time and there are two elements with peak values in the circumferential direction, and

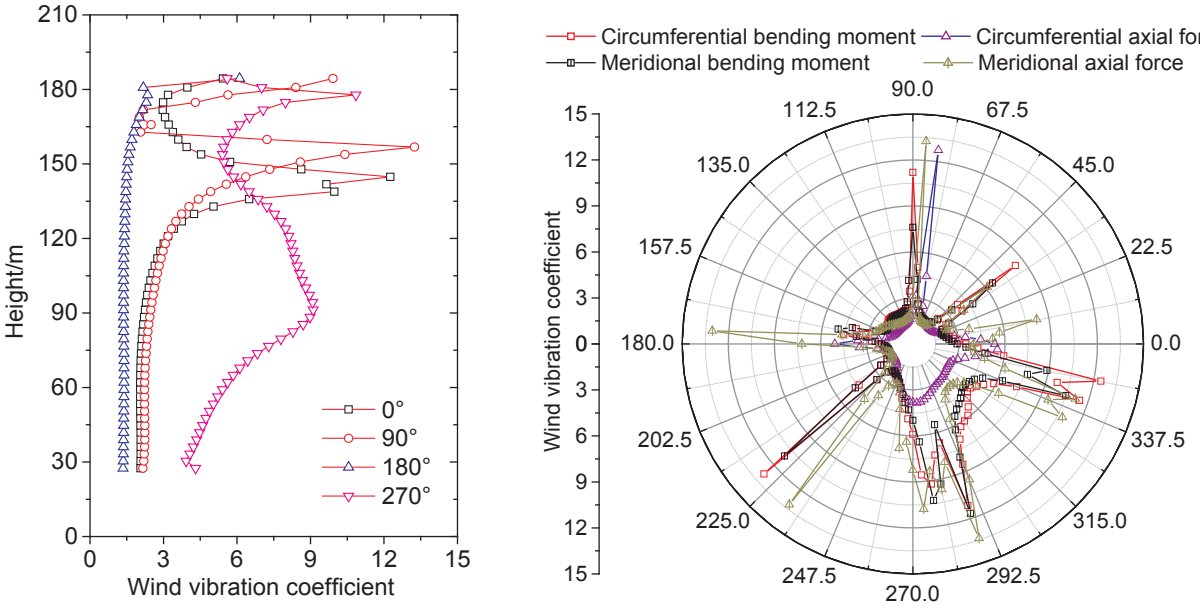

a) Wind-induced vibration coefficients based on circular bending moment

b) Wind-induced vibration coefficients with different definition in throat

Fig. 16. Variety of wind-induced vibration coefficients in level of internal force.

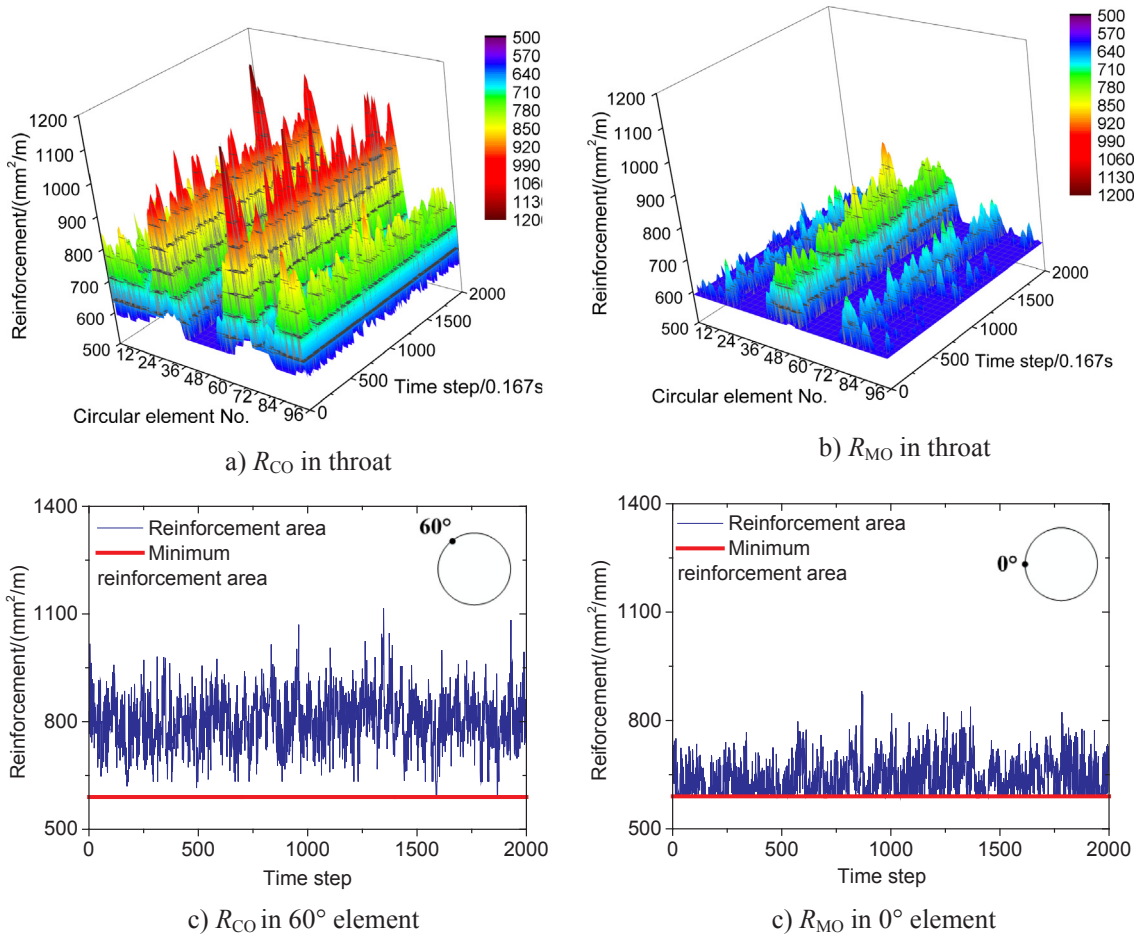

a) R_{CO} in throat

b) R_{MO} in throat

c) R_{CO} in 60° element

c) R_{MO} in 0° element

Fig. 17. Time-variant dynamic reinforcement area in throat.

their relative angles with respect to wind direction are around 60° and 300°. The results show that the circumferential reinforcement area is greater on the lateral wind surface than in other parts.

As seen in Fig. 17(b), in the meridional direction, the time-variant reinforcement area is also complicated. The reinforcement area reaches a peak value on the windward side, and the second largest value is on the lateral wind surface. Therefore, the reinforcement area is asymmetric in the circumferential direction with interference effect. The circumferential reinforcement area is determined by the lateral wind surface, and for the meridional reinforcement area it is determined by the windward side.

7. Overall tower structural safety evaluation

The envelope for maximal reinforcement area can be used as the overall structural design criterion and to evaluate tower group interference effects. It can comprehensively include various factors, such as IF and wind-induced vibration coefficients. The results obtained through this criterion comprehensively show the structural wind-induced dynamic performance for tower group interference conditions. At the same time, the reinforcement area envelope as a criterion must consider the influence of interferences for different inflow wind directions, differences in circumferential reinforcement area, and even edge effects to ensure that the criteria are comprehensive and reasonably adjusted to structural strength design. Through calculation of the reinforcement area in each element over time by the peak factor introduced in Eq. (11) above, the reinforcement area envelope value of each element over time can be obtained.

From Eq. (12), the maximum values of reinforcement area extreme values of all elements in the circumferential direction are calculated first. At this point the reinforcement area envelope line along the height for the “narrow channeling” condition can be built. To analyze the reinforcement area of the entire tower for this most unfavorable condition, wind directions other than 180°for the “narrow channeling” condition should be calculated. The outer envelope line is taken as the evaluation criterion. Fig. 18 shows the reinforcement envelope in the meridional and circumferential directions at inner and outer tower surfaces for different wind directions.

It can thus be concluded that the circumferential reinforcement areas at both inner and outer tower surfaces change insignificantly for different wind directions, but the meridional reinforcement area is strongly affected by wind direction. Generally, for all 4 cases, the maximum reinforcement area in T3 tower lies between 180° and 225° in the rhombus arrangement, and the minimum value appears in the 90° wind direction. This shows that the leeward side is more unfavorable to rhombus-arranged tower groups. The fluctuating loads on the windward side control the meridional reinforcement. Tower group interference has a significant effect on pulsating loads and its dynamic reinforcement area compared with the isolated tower.

Nevertheless, cooling tower structures were designed according to three different current codes [23,24]. These codes over-simplify the analysis of wind loads on cooling towers, and are not suitable for current super-large cooling towers with complex interference effects. In Fig. 19, the code results are compared with those of the dynamic reinforcement method with interference effects and the isolated tower dynamic reinforcement area envelope line. For the codes, the wind-induced vibration coefficient is set as 1.9, and that of IF is 1.0.

It can be concluded that, under tower group interference conditions,

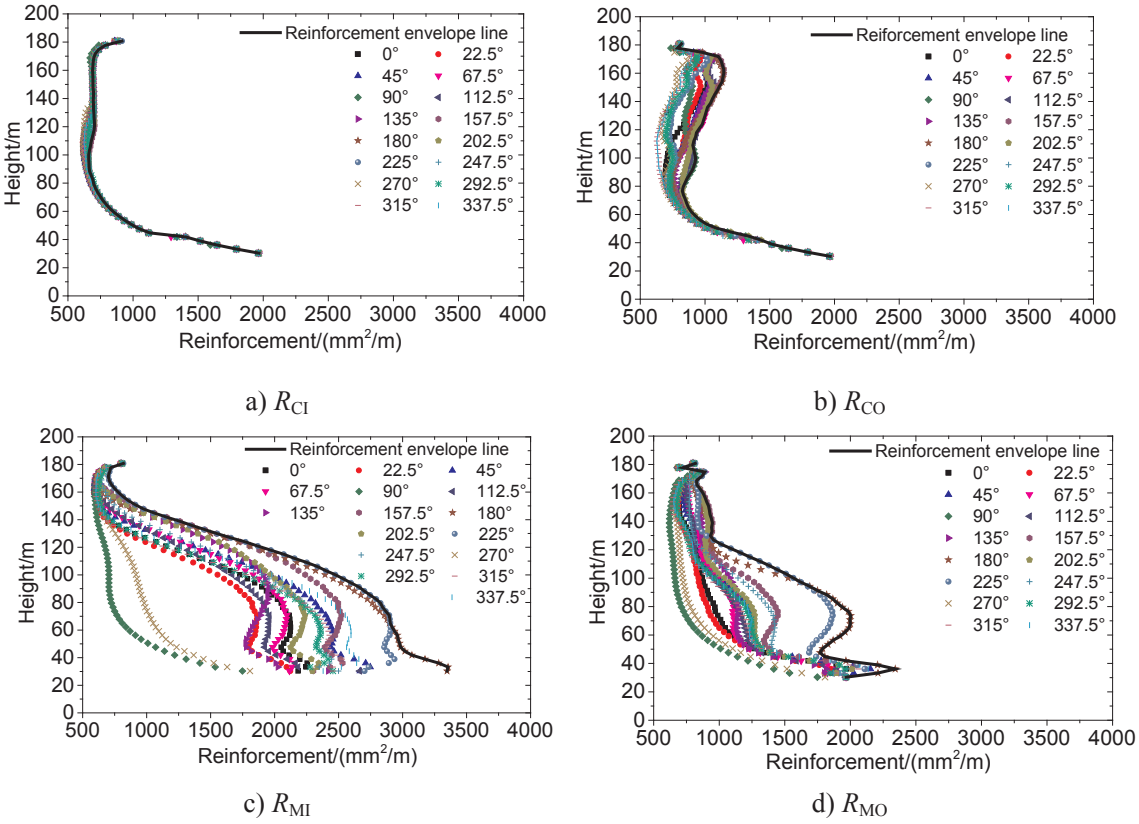

Fig. 18. Reinforcement area envelopes for various incoming wind direction.

the interference affects, both the average wind pressure and the fluctuating wind pressure, result in a larger and more complex reinforcement area envelope than that for an isolated tower. In the lower part of the tower, R_{MI} and R_{MO} are significantly increased. In the upper part of the tower, R_{CO} is significantly increased. For other conditions, all reinforcement areas vary little over the entire tower.

Comparing the tower reinforcement area envelope with interference effects and the equivalent reinforcement obtained from code methods, it is found that the meridional reinforcement obtained from the code methods is insufficient to carry the larger fluctuating wind pressures on the windward side at the upper level, because the meridional reinforcement area is determined by the pressures on the windward side surface. However, the reinforcement is adequate in the middle and lower part of the tower. For circumferential reinforcement, the R_{CO} obtained from all codes except the VGB code are reasonable. The R_{CI} obtained from most codes will be significantly insufficient in some areas, but that obtained from the VGB code meets the safety requirement.

This means that the two-dimensional static wind pressure distribution method proposed by the codes ignores asymmetrical effects of wind pressure with interference effects, which is unsafe for structural design, especially for large-scale cooling towers. It is reasonable to adopt 3-D equivalent wind loads to derive a reinforcement area envelope to ensure both safety and economy of the structure. Based on the results of this example, it is concluded that the current codes are inaccurate and unsafe for several specific structural parts. For other parts, the reinforcement envelope method based on the dynamic reinforcement area extreme values can greatly reduce the redundant reinforcement through optimized 3-D ESWL.

Furthermore, the existing problems in cooling tower structural design, such as complexity of internal force criteria and abnormal values of wind loading factors from GLF, are also solved. By analyzing the tower group interference effects and structural vibration responses using the reinforcement envelope criterion, an optimal solution to wind-induced structural performance can be achieved.

8. Conclusions

Through wind tunnel tests, FEM model dynamic force calculation and internal force-weighted structural reinforcement area, a reinforcement envelope strategy for a rhombus-arranged eight-tower group was implemented. The variation regulations for reinforcement area for cooling tower structures under tower group interference conditions were summarized. Some detailed conclusions are listed below:

(1) Due to tower group interference effects, the symmetry of the average wind pressure is obviously changed, and the fluctuating wind pressure is significantly increased for most parts. This phenomenon is more noticeable on the windward side, and the upper parts of the tower usually suffer stronger loading actions than the lower ones.
(2) The effect of wind fluctuations cannot be ignored. At the dynamic reinforcement level, this effect is not only present on the windward side, but also has a significant impact on the lateral and leeward areas. For the same tower height, extreme values of circumferential reinforcement are required on the lateral wind parts, and extreme values of meridional reinforcement are concentrated on the windward sides.
(3) Under conditions of tower group interference, the dynamic reinforcement area shows a non-linear amplification compared with that for an isolated tower due to the complex influence of average and fluctuating wind pressures. It is proposed to adopt spatial equivalent static wind loads through the reinforcement criterion rather than the traditional amplified 2-D symmetric wind load, which is more accurate and consistent with the structural characteristics of the cooling tower, to ensure the safety and economy of

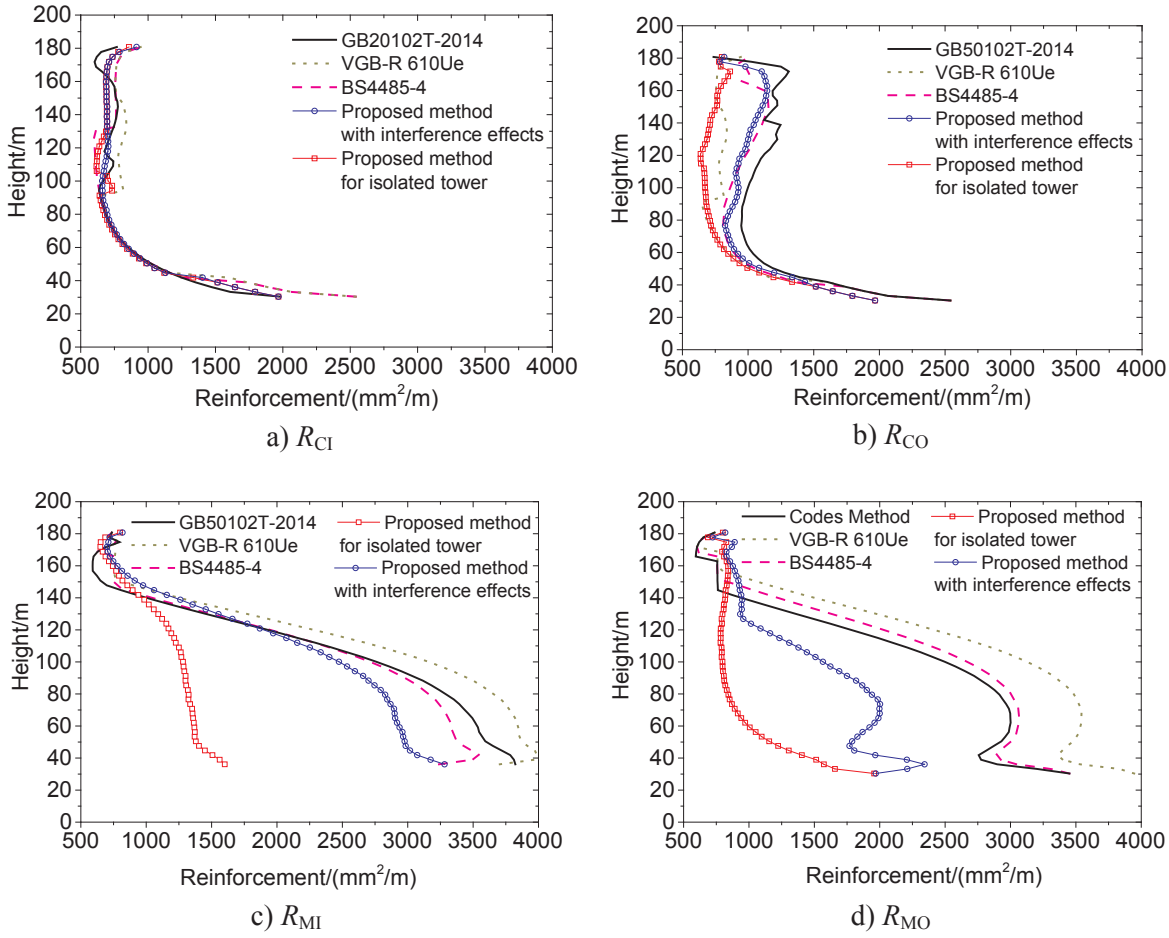

Fig. 19. Comparison of reinforcement area envelope under conditions of wind tunnel experiments and codes.

structural design.

(4) Using the dynamic reinforcement area envelope criterion, an improved method for quantifying the tower group interference effects and structural vibration effects is proposed, which can accurately analyze structural performance and thus avoid structural material waste compared with simplified wind loading factors. The reinforcement area envelope criterion can be employed as a reasonable method for both direct structural design and ESWL calculation.

Acknowledgements

The authors gratefully acknowledge the support of the National Key Research and Development Program of China (2018YFC0809600, 2018YFC0809604) and the National Natural Science Foundation of China (51678451).

Appendix A. Supplementary material

Supplementary data to this article can be found online at https://doi.org/10.1016/j.engstruct.2019.05.031.

References

[1] Armitt J. Wind loading on cooling towers. J Struct Div 1980;106(3):623–41.
[2] Pope RA. Structural deficiencies of natural draught cooling towers at UK power stations. Part 1: failures at Ferrybridge and Fiddlers Ferry. Proc ICE Struct Build 1994;104(1):1–10.
[3] Sun TF, Gu ZF. Interference between wind loading on group of structures. J Wind Eng Ind Aerodyn 1995;54:213–25.
[4] Niemann HJ, Kopper HD. Influence of adjacent buildings on wind effects on cooling towers. Eng Struct 1998;20:874–80.
[5] Orlando M. Wind-induced interference effects on two adjacent cooling towers. Eng Struct 2001;23:979–92.
[6] Zhao L, Chen X, Ke ST, Ge YJ. Aerodynamic and aero-elastic performances of super-large cooling towers. Wind Struct 2014;19:443–65.
[7] Ke ST, Zhao L, Ge YJ, Chen SL. Wind-induced responses of super-large cooling towers. J Central South Univ 2013;20(11):3216–28.
[8] Uematsu Y, Koo C, Yasunaga J. Design wind force coefficients for open-topped oil storage tanks focusing on the wind-induced buckling. J Wind Eng Ind Aerodyn 2014;130:16–29.
[9] Zhang JF, Ge YJ, Zhao L, Zhu B. Wind induced dynamic responses on hyperbolic cooling tower shells and the equivalent static wind load. J Wind Eng Ind Aerodyn 2017;169:280–9.
[10] Zhao L, Zhan YY, Ge YJ. Wind-induced equivalent static interference criteria and its effects on cooling towers with complex arrangements. Eng Struct 2018;172:141–53.
[11] GB50102T-2014. Code for hydraulic design of fossil fuel power plants. Beijing: China Architecture and Building Press; 2014.
[12] Katsumura A, Tamura Y, Nakamura O. Universal wind load distribution simultaneously reproducing largest load effects in all subject members on large-span cantilevered roof. J Wind Eng Ind Aerodyn 2007;95(9–11):1145–65.
[13] Holmes JD, Sankaran R, Kwok KCS, et al. Eigenvector modes of fluctuating pressures on low-rise building models. J Wind Eng Ind Aerodyn 1997;69:697–707.
[14] GB50010-2010. Code for design of concrete structures. Beijing: China Architecture and Building Press; 2010.
[15] Davenport AG. Gust loading factors. J Struct Div 1967;93(3):11–34.
[16] Ke ST, Ge YJ, Zhao L. Research on features of fluctuating wind pressure on large hyperbolic cooling tower: features of non-Gaussian. J Exp Fluid Mech 2010;24(3):12–8.
[17] Simiu E. Wind spectra and dynamic alongwind response. J Struct Div 1974;100(9):1897–910.
[18] Hu CX, Zhao L, Ge YJ. Time-frequency evolutionary characteristics of aerodynamic forces around a streamlined closed-box girder during vortex-induced vibration. J Wind Eng Ind Aerodyn 2018;182:330–43.
[19] Zhao L, Ge YJ, Kareem A. Fluctuating wind pressure distribution around full-scale cooling towers. J Wind Eng Ind Aerodyn 2017;165:34–45.
[20] JTG D63-2007. Code for design of ground base and foundation of highway bridges and culverts. Beijing: China Architecture and Building Press; 2007.
[21] Zhao SY, Chen NY, Zhao L, Ge YJ. Wind-induced response resonance component and its effects of large steel structure cooling tower. The 4th national structural wind engineering graduate forum. 2017. p. 403–4. [in Chinese].
[22] Lee BJ, Gould PL. Seismic response of pile supported cooling towers. J Struct Eng 1985;111(9).
[23] BS 4485-4. Code of practice for structural design and construction-Water cooling tower. London: British Standard Institution; 1996.
[24] VGB-R 610Ue. Structural design of cooling towers. German: VGB Power Tech e.V; 2005.